# Bi-dimensional simulation of MOSFET's in thermal equilibrium

Guido Araújo*, Petrônio Pulino**, Bernard Waldman***

Department of Computer Science - DCC/IMECC(*)
Laboratory of Electronics and Devices - DEMIC/FEE(*)(***)
Department of Applied Mathematics - DMAC/IMECC(**)
UNICAMP, Cid. Universitária Zeferino Vaz, Campinas - SP, 13801
bitnet e-mail guido@bruc.ansp.br

## ABSTRACT

The rapid increase in the development of new VLSI structures indicates that the most cost effective way to design semiconductor devices is using numerical simulation based on sophisticated bi or three-dimensional models. In this paper we detail the solution of the bi-dimensional Poisson equation applied to a MOSFET in thermal equilibrium. This problem, although quite simple, can give detailed information about the operation of sub-micron devices in certain conditions, and serves as a good introduction to the study of the dimensional effects in the operation of semiconductor structures. We obtain numerical results and establish some comparisons between devices with channels length of $5.0\mu m$ and $1.0\mu m$.

## 2. INTRODUCTION

The technological process used in the design of semiconductor devices has been traditionally based on experimental techniques. In a general manner, the design of the device begins with a poor analytical approach to the device structure. After that, a great number of interation steps in fabrication, characterization and redesign is executed, until an adequate performance for the device is obtained. Once the design goal is obtained, some *design-rules* are derived for use in the design of future devices.

With the advent of new and more complex VLSI devices, the number of design/fabrication interation steps increased in such a way, that the traditional design process became expensive and time consuming. In the last few years a new methodology, based on numerical simulation of sophisticated physical models, has been proved to be a reliable and inexpensive solution for this problem.

In the development of a new CMOS device, for example, the fabrication and characterization steps of a real experiment could take weeks or even months. In the other hand, the numerical simulation of this process, takes only some hours or days. Some authors estimate a final cost reduction of 40%, if it is used numerical simulation during the complete design[1]. A great number of software packages using simulation techniques for semiconductor devices has been developed. We mention, for example, SUPREM[2] used in simulation of fabrication steps and MINIMOS[3], FIELDAY[4], for the simulation of device operation. The device operation simulation programs use, in different ways, simulation techniques based on the early semiconductors simulation papers by Gummel[5], De Mari[6], Sharffeter[7], Mock[8], and others.

In this article we describe with details, the bi-dimensional solution of the Poisson equation in thermal equilibrium MOSFET, trying to focus the dimensional effects in the electrical potential distribution $\psi$, resulting from the drastic reduction of the device channel length.

We begin in Sec.3 describing the determination of a bi-dimensional profile produced by implantation and diffusion of dopants in the drain and source regions. In Sec.4 we derive the discretization of Poisson equation, using finite-difference techniques, and we formulate the discretized boundary conditions. In Sec.5 we describe the numerical treatment, and in Sec.6 we present two simulation examples.

## 3. BI-DIMESIONAL DOPING PROFILE

Generally, the doping process used in the fabrication of a semiconductor device is based on a sequence of implantation and *drive-in* steps. The determination of an analytical solution for a bi-dimensional doping profile can be obtained by solving the diffusion equation.

$$\frac{\partial I}{\partial t} = D.\left\{\frac{\partial^2 I}{\partial x^2} + \frac{\partial^2 I}{\partial y^2}\right\} \tag{1}$$

In (1), t is the diffusion time, D is the diffusion coefficient in the diffusion temperature, and $I(x,y,t)$, the doping distribution of the implanted dopants during diffusion. For the solution of (1) in an inert environment, we suppose that no inter-diffusion of dopants occur in the semiconductor surface:

$$\left.\frac{\partial I}{\partial y}\right|_{y=0} = 0 \tag{2}$$

A first approach solution of (1) may be obtained approximating the implant profile by a unit impulse function:

$$I(x',y',0) = \delta(x',y') \tag{3}$$

The solution of (1) in the domain $x \in [-\infty,+\infty], y \in [0,+\infty]$, with initial condition (3) and boundary condition (2), is a classical result[9]:

$$\begin{aligned} I_\delta(x,y,t) &= \frac{1}{2\pi Dt}\exp\left(-\frac{(x-x')^2}{4Dt}\right)\left[\exp\left(-\frac{(y-y')^2}{4Dt}\right)\right. \\ &\left. + \exp\left(-\frac{(x+x')^2}{4Dt}\right)\right] \end{aligned} \tag{4}$$

Using (4), the solution of (1) for an arbitrary initial condition $I_0(x',y',0)$ can be obtained using convolution:

$$I(x,y,t) = \int_0^{+\infty}\int_{-\infty}^{+\infty} I_0(x',y',0).I_\delta(x,y,t)\,dx'\,dy' \tag{5}$$

Consider now a Gaussian distribution with no lateral spreading, as a reasonable approximation for the initial implanted profile. The implantation done on a silicon surface, through an infinite mask which edge is positioned at x = a :

$$I_0(x',y',0) = \begin{cases} 0 & x < a \\ \frac{I_{max}}{\sqrt{2\pi}\sigma_p}.\exp\left(-\frac{(y-R_p)^2}{2\sigma_p^2}\right) & x \geq a \end{cases}$$

In the above function $I_{max}$ is the maximum concentration, $R_p$ is the implant projected range, $\sigma_p$ is the standard deviation. Substituting this function into (5) we obtain, after some algebra, an analytical bi-dimensional profile, resulting from a ***drive-in*** diffusion of a Gaussian distribution in the semiconductor. This approach was first investigated by Lee[10], who refined it after taking in account lateral spread[11].

$$I(x,y,t) = \frac{I_{max}}{4\pi Dt} I_x(x,t).I_y(y,t) \tag{6}$$

where,

$$I_x(x,t) = \frac{1}{\sqrt{2\pi}\sigma_p}.\mathrm{erfc}\left(\frac{x-a}{2\sqrt{Dt}}\right) \tag{7}$$

$$I_y(y,t) = \Omega(y,t) + \Omega(-y,t) \tag{8}$$

$$\begin{aligned} \Omega(y,t) &= \sigma_p.\sqrt{\frac{Dt\pi}{2Dt+\sigma_p^2}}\mathrm{erfc}\left[-\frac{R_p}{\sigma_p}.\sqrt{\frac{Dt}{2Dt+\sigma_p^2}} - \sqrt{\frac{\sigma_p^2}{4Dt(2Dt+\sigma_p^2)}}y\right]. \\ &\exp\left(-\frac{(y-R_p)^2}{2\sigma_p^2+4Dt}\right) \end{aligned} \tag{9}$$

We note that the final distribution (6) is a product of two uncoupled distributions, a vertical profile $I_y$ and a lateral profile $I_x$. The Equation (6) was implemented numerically, using a numerical approximation to the function erfc, and a polinomial approximation to estimate $R_p$ and $\sigma_p$ as a function of the implanting energy[12]. The diffusion coefficient $D$ is determined using Arrhenius formulation.

## 4. DISCRETIZATION OF POISSON EQUATION

The classical Poisson equation relates the divergence of the electrical field vector $\vec{E}$ to the charge density $\rho$:

$$div\vec{E} = \frac{\rho}{\epsilon} \tag{10}$$

,where $\epsilon$ is the electrical permittivity. The model we use for MOSFET device in this section assumes some approximations, which permit the solution of the Poisson equation, with a good accuracy. These approximations are : parabolic band structure with nondegenerate semiconductor, which permits the carrier densities $n$ and $p$ to be derived in thermal equilibrium conditions by Boltzmann statistics.

In order to simplify the numerical problem, let us take the *fermi-level* potential as the electrical potential reference, and normalize the problem variables. The potential is normalized[6] by the thermal voltage ($kT/q$), the charge density by the electron charge $q$, and the carrier density by the intrinsic concentration ($n_i$). This reduces the Boltzmann carrier concentrations to:

$$n = e^{\psi} \tag{11}$$

$$p = e^{-\psi} \tag{12}$$

In the discretization of Equation (10) we use finite-difference techniques, since its convergence properties are well established. The device domain $R$ is divided in small rectangular subdomains $\partial R_{ij}$ by a mesh $M = \{(x_i, y_j), 1 \leq i \leq n_x, 1 \leq i \leq n_y\}$ formed by the interception of $n_x$ lines parallel to axis $y$ and $n_y$ lines parallel to axis $x$. This mesh cannot be choosen arbitrarialy, since its density must be adequate to the potential variations along the device. In regions where rapid potential variations occur (vicinity of drain, source and interface $Si - SiO_2$) the mesh should be much more dense than in regions where the potential behavior is smooth (substrate, for example).

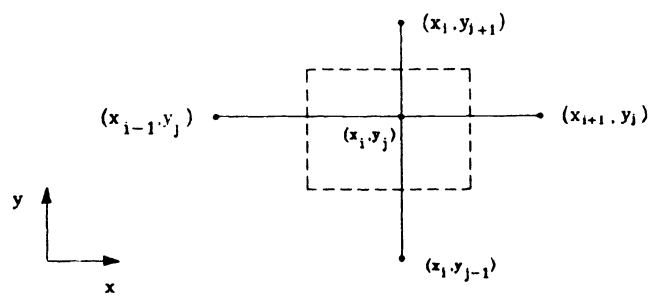


Figure 1: Subdomain $\partial R_{ij}$ and its five points system

Each interception point $(x_i, y_j)$ of mesh $M$, has four neighbors points named $(x_{i+1}, y_j)$, $(x_{i-1}, y_j)$, $(x_i, y_{j-1})$ and $(x_i, y_{j+1})$ (Fig. 1). The distance of point $(x_i, y_j)$ to its four neighbors may be expressed as:

$$h_i = x_i - x_{i-1} \tag{13}$$

$$h_{i+1} = x_{i+1} - x_i \tag{14}$$

$$k_j = y_j - y_{j-1} \tag{15}$$

$$k_{j+1} = y_{j+1} - y_j \tag{16}$$

The subdomain $\partial R_{ij}$ ,where the Poisson equation will be discretized, consists of a rectangular region inside the broken line of the Fig. 1. The sides of the rectangle intercept the mesh lines in midpoints:

$$x_{i+1/2} = (x_{i+1} + x_i)/2 \tag{17}$$

$$x_{i-1/2} = (x_i + x_{i-1})/2 \tag{18}$$

$$y_{j-1/2} = (y_j + y_{j-1})/2 \tag{19}$$

$$y_{j+1/2} = (y_{j+1} + y_j)/2 \tag{20}$$

Integrating equation (10) over the subdomain $\partial R_{ij}$, and applying the Divergence Theorem we obtain:

$$\oint_{\partial C_{ij}} E_x\, dy - E_y\, dx = \int\int_{\partial R_{ij}} \frac{\rho}{\epsilon}\, dx\, dy \tag{21}$$

The left member of (21) is a line integral over the boundary $\partial C_{ij}$ of the subdomain $\partial R_{ij}$, where $E_x$ and $E_y$ are the electrical field components. Firstly, we concentrate our attention to the left member of (21). Observing Fig. 1 we note that the line integral around the boundary $\partial C_{ij}$ is equal to the sum of four line integrals corresponding to the sides of the rectangle. Consequently we can define the left member of (21) as:

$$M_l = \sum_{k=1}^{4} \int_{\partial C_{ij}^k} E_x\, dy - E_y\, dx = \sum_{k=1}^{4} I_k \tag{22}$$

and the right member as:

$$M_r = \int\int_{\partial R_{ij}} \frac{\rho}{\epsilon}\, dx\, dy \tag{23}$$

In the Equation (22), $\partial C_{ij}^k$ corresponds to the side $k$ of the boundary rectangle $\partial C_{ij}$. The side enumeration begins with the side that contains the point $(x_{i+1}, y_j)$, defined as $\partial C_{ij}^1$, and continues counterclockwise until $\partial C_{ij}^4$. The integrals $I_k$ may be expressed as:

$$I_1 = \int_{y_j - k_j/2}^{y_j + k_{j+1}/2} E_x\, dy \tag{24}$$

$$I_2 = -\int_{x_i + h_{i+1}/2}^{x_i - h_i/2} E_y\, dx \tag{25}$$

$$I_3 = \int_{y_j + k_{j+1}/2}^{y_j - k_j/2} E_x\, dy \tag{26}$$

$$I_4 = -\int_{x_i - h_i/2}^{x_i + h_{i+1}/2} E_y\, dx \tag{27}$$

The approximations for the integrals $I_k$ in the integration paths must be done with care. We suppose that the variations of the electrical field components $E_x$ and $E_y$ in each side $\partial C_{ij}^k$ are sufficiently smooth, what permits to consider them constant in this region. We should again emphasize, that this assumption will be valid , if we could have an enough dense mesh in regions with rapid potential variations. If that is the case, we can approximate the electrical components by their values in the midpoints defined in (17) - (20). The integrals $I_k$ take the appoximate form $\overline{I_k}$:

$$\begin{aligned} \overline{I_1} &= E_x(x_{i+1/2}, y_j).\Delta y \\ &= E_x(x_{i+1/2}, y_j).[(y_j + k_{j+1}/2) - (y_j - k_j/2)] \\ &= E_x(x_{i+1/2}, y_j).(k_{j+1} + k_j)/2 \end{aligned} \tag{28}$$

$$\begin{aligned} \overline{I_2} &= -E_y(x_i, y_{j+1/2}).\Delta x \\ &= -E_y(x_i, y_{j+1/2}).[(x_i - h_i/2) - (x_i + h_{i+1}/2)] \\ &= E_y(x_i, y_{j+1/2}).(h_{i+1} + h_i)/2 \end{aligned} \tag{29}$$

$$\begin{aligned}\overline{I_3} &= E_x(x_{i-1/2}, y_j).\Delta y \\ &= E_x(x_{i-1/2}, y_j).[(y_j - k_j/2) - (y_j + k_{j+1}/2)] \\ &= -E_x(x_{i-1/2}, y_j).(k_{j+1} + k_j)/2 \end{aligned} \tag{30}$$

$$\begin{aligned}\overline{I_4} &= -E_y(x_i, y_{j-1/2}).\Delta x \\ &= -E_y(x_i, y_{j-1/2}).[(x_i + h_{i+1}/2) - (x_i - h_i/2)] \\ &= -E_y(x_i, y_{j-1/2}).(h_{i+1} + h_i)/2 \end{aligned} \tag{31}$$

The next step in the problem of discretizing (22), is the determination of approximations for the electrical field components, functions of the electrical potential, in the boundary $\partial C_{ij}$. Since we supposed a constant electrical field along the integration paths $\partial C_{ij}^k$, it is reasonable to obtain the midpoints values of the electrical components, using central interpolation of the potential $\psi$ ($\vec{E} = -grad\,\psi$):

$$E_x(x_{i+1/2}, y_j) = -(\psi_{i+1,j} - \psi_{i,j})/h_{i+1} \tag{32}$$

$$E_y(x_i, y_{j+1/2}) = -(\psi_{i,j+1} - \psi_{i,j})/k_{j+1} \tag{33}$$

$$E_x(x_{i-1/2}, y_j) = -(\psi_{i,j} - \psi_{i-1,j})/h_i \tag{34}$$

$$E_y(x_i, y_{j-1/2}) = -(\psi_{i,j} - \psi_{i,j-1})/k_j \tag{35}$$

Substituting (32) - (35) and (28) - (31) into (22) we obtain a discretized equation correspondent to $M_l$.

We should now determine the discretization of the right member of (21). Supposing again that the sub-domain $\partial R_{ij}$ is sufficiently small, we can approximate $M_r$ by:

$$\overline{M_r} = \frac{\rho(x_i, y_j)}{\epsilon}.A_{\partial R_{ij}} \tag{36}$$

,where $A_{\partial R_{ij}}$ represents the area of the subdomain rectangle $\partial R_{ij}$, and $\rho(x_i, y_j)$, the value of the charge density in the point $(x_i, y_j)$. According to Fig.1 the rectangular domain area is $A_{\partial R_{ij}} = (h_i/2 + h_{i+1}/2).(k_j/2 + k_{j+1}/2)$. Substituting $A_{\partial R_{ij}}$ into (36), we obtain the discrete equation for $M_r$:

$$\overline{M_r} = \frac{\rho(x_i, y_j)}{\epsilon}.(h_i + h_{i+1}).(k_j + k_{j+1})/4 \tag{37}$$

Once derived $M_l$ and $\overline{M_r}$, we finally obtain the discretized Poisson equation, in a point $(x_i, y_j)$ inside the MOSFET device:

$$\begin{aligned}\psi_{i,j}.\left(\frac{h_i + h_{i+1}}{h_i h_{i+1}}(k_j + k_{j+1}) + \frac{k_j + k_{j+1}}{k_j k_{j+1}}(h_i + h_{i+1})\right) - \psi_{i-1,j}.\left(\frac{k_j + k_{j+1}}{h_i}\right) \\ -\psi_{i+1,j}.\left(\frac{k_j + k_{j+1}}{h_{i+1}}\right) - \psi_{i,j-1}.\left(\frac{h_i + h_{i+1}}{k_j}\right) - \psi_{i,j+1}\left(\frac{h_i + h_{i+1}}{k_{j+1}}\right) \\ = \frac{\rho(x_i, y_j)}{2\epsilon}.(h_i + h_{i+1})(k_j + k_{j+1})\end{aligned} \tag{38}$$

## 5. BOUNDARY CONDITIONS

The domain of a typical MOSFET device has a rectangular structure, like that in the Fig. 2. In a general manner, we can divide the boundaries of this structure in three categories: ohmic contacts (BC, DE and FA), artificial boundaries (AB and EF) and semiconductor-oxide interface (CD). Each category contributes with a different type boundary condition, that is derived by physical and mathematical reasoning. In the following explanations we obtain discretized equations for these boundary conditions.

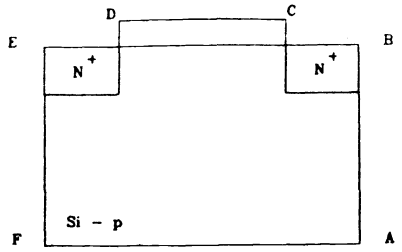


Figure 2: MOSFET device structure

5.1 Ohmic contacts

Let us suppose that the ohmic contacts of source (DE), drain (BC) and bulk (AF) are ideal. This can be physically expressed, supposing that in the surface contact we have *space-charge neutrality* ($\rho = 0$) and *thermal equilibrium* (corresponding to infinite surface recombination). With the carrier density normalized:

$$n_{i,j}p_{i,j} = 1 \tag{39}$$

$$n_{i,j} - p_{i,j} - N_{i,j} = 0 \tag{40}$$

,where N is the dopant concentration. In the above equations, the indices $i$ and $j$ indicate that the values of $n$,$p$ and $N$ are considered at the point $(x_i, y_j)$ of the ohmic contact. The solution of equations (39) - (40), together with the Boltzmann approximations for the carrier densities, produce a Dirichlet boundary condition to the potential at the point $(x_i, y_j)$:

$$\psi_{i,j} = \ln\left(\frac{N_{i,j}}{2} + \sqrt{\frac{N_{i,j}^2}{4} + 1}\right) \tag{41}$$

5.2 Artificial boundaries

The artificial boundaries (AB) and (EF) ,Fig. 2, are not real boundaries in the physical sense. They are introduced in order to isolate the device domain in a closed form, enabling its simulation. The conditions associated with these boundaries can be derived by a previous qualitative knowledge of the device operation.

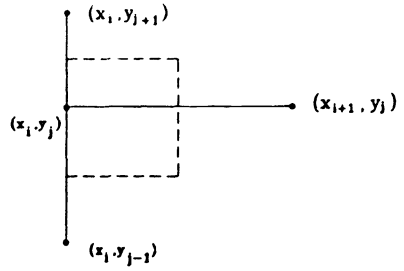


Figure 3: Artificial boundary (EF)

A natural manner to isolate the device is to suppose that the potential derivatives vanish in a direction perpendicular to the artificial boundary. This is formulated by a Neumann boundary condition:

$$\frac{\partial \psi}{\partial \vec{n}} = 0 \tag{42}$$

,where $\vec{n}$ is a unitary vector perpendicular to the artificial boundary. The discretization of equation (42) at the point $(x_i, y_j)$ (Fig.3) on the artificial boundary (EF) is:

$$\left.\frac{\partial \psi}{\partial x}\right|_{x_i,y_j} = 0 \tag{43}$$

$$\psi_{i+1,j} - \psi_{i,j} = 0 \tag{44}$$

These formulations can be identically applied to the boundary (AB).

5.3 Semiconductor-oxide interface

In the semiconductor-oxide interface we have the discretized electrical potential equation by applying the Gauss law. Supposing that the electrical field vector is predominantly vertical in the semiconductor-oxide interface:

$$\epsilon_s \frac{\partial \psi_s}{\partial y} - \epsilon_o \frac{\partial \psi_o}{\partial y} = Q_{int} \tag{45}$$

,where $Q_{int}$ is the interface trapped charge, $\epsilon_s$ and $\epsilon_o$ denote the silicon and the oxide electrical permittivities respectively, and $\psi_s$ and $\psi_o$ the electrical potentials.

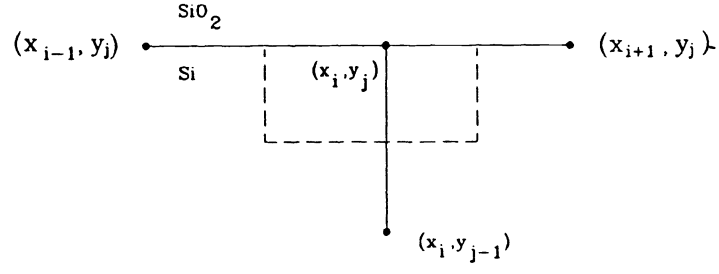


Figure 4: Interface discretization

The problem now is to determine the potential $\psi_o$ in the oxide. For simplicity, we suppose that the oxide region is free of electrical charge. This assumption lead us to consider the validity of Laplace equation inside the oxide. Therefore, the electrical field (i.e. its vertical component $E_y$), can be considered constant. Since the thickness ($t_{ox}$) of the oxide layer is very thin, we can approximate $E_y$ by:

$$E_y = -\frac{\partial \psi_o}{\partial y} \approx \frac{\psi_s - V_g}{t_{ox}} \tag{46}$$

,where $V_g$ is the gate potential. Substituting (46) into (45) and denoting the semiconductor potential by $\psi$, instead of $\psi_s$, we have:

$$\frac{\partial \psi}{\partial y} + \frac{\epsilon_o}{\epsilon_s t_{ox}}\psi = \frac{Q_{int}}{\epsilon_s} + \frac{\epsilon_o}{\epsilon_s t_{ox}} V_g \tag{47}$$

According to Fig. 4, the vertical electrical field component $\frac{\partial \psi}{\partial y}$ can be approximated by:

$$\frac{\partial \psi}{\partial y} \approx \frac{\psi_{i,j} - \psi_{i,j-1}}{k_j} \tag{48}$$

Substituting the above approximation above in (47), we derive the discretized interface equation:

$$\psi_{i,j}\left(\frac{1}{k_j} + \frac{\epsilon_o}{\epsilon_s t_{ox}}\right) - \psi_{i,j-1}\frac{1}{k_j} = \frac{Q_{int}}{\epsilon_s} + \frac{\epsilon_o}{\epsilon_s t_{ox}} V_g \tag{49}$$

In the discretization of Poisson equation (10) we did not make any consideration about the linearization of the space charge density $\rho$, which in a normalized form is:

$$\rho = p - n + N \tag{50}$$

$$\rho(\psi) = e^{-\psi} - e^{\psi} + N \tag{51}$$

This can be done now, if we take a first order approach for $\rho$ in the neighborhood of the point $(x_i, y_j)$:

$$\rho(\psi) \approx \rho(\psi_{i,j}) + \rho'(\psi_{i,j})(\psi - \psi_{i,j}) \tag{52}$$

,where $\rho'(\psi_{i,j})$ is the charge density derivative at the point $(x_i, y_j)$. Substituting (52) into the Poisson equation (10) we have:

$$\epsilon_s \Delta\psi + \rho'(\psi_{i,j})\psi = \rho'(\psi_{i,j})\psi_{i,j} - \rho(\psi_{i,j}) \tag{53}$$

,where $\Delta\psi$ is the Laplacian of the electrical potential. The conventional approach to the numerical solution of the Equation (53) is based on the application of Newton method. Let us take the potential $\psi$ in (53), as the potential value in the next Newton interation step. Therefore the Equation (53), can be written:

$$\epsilon_s \Delta\psi^{k+1} + \rho'(\psi^k_{i,j})\psi^{k+1} = \rho'(\psi^k_{i,j})\psi^k_{i,j} - \rho(\psi^k_{i,j}) \tag{54}$$

,where the indices $k+1$ and $k$ correspond to the number of the Newton interation step. The discretization of the Laplacian $\Delta\psi^{k+1}$ was done in the left member of equation (38) of Sec.4.

Finally, the solution of the algebric linear system resulting from each Newton interation step can be obtained by Gauss-Siedel method with SOR (Succesive Overrelaxation) acceleration technique.

## 7. EXAMPLES

In this section we want to present some illustrative examples of Poisson bi-dimensional simulations performed in two n-channel MOSFET devices with $5.0\mu m$ and $1.0\mu m$ channel lengths. In both devices we used a substrate doping of $10^{16} cm^{-3}$, source-drain implantation with phosphorus, with implantation dose of $10^{16} cm^{-2}$ and implantation energy of $40\,keV$. The implantation is done through a free silicon surface, and the *drive-in* step is performed at $1000\,^{\circ}C$ for $900\,s$. Although more realistic doping profiles could be used, by employing process simulation programs like SUPREM[2], we consider that the profile derived in Sec. 3 is enough accurate to our purpose. For the gate characteristics we considered an oxide thickness of $500\,\AA$, gate material Aluminium and zero interface charge density.

Because of the drain and source lateral subdiffusion, we note from Fig.5, that the p-n junction is positioned approximately at $0.3\mu m$ from the mask edge. This results in an effective channel length of $0.4\mu m$. From Figs.6 - 7 we observe the potential distribution in the devices, when the gate voltage applied to them is approximately the long-channel device threshold voltage. It is well known, and we can check in these figures, that the short-channel device performs the channel inversion before the long-channel device, which contributes to the decreasing of the threshold voltage value in very small MOSFET's. We want to emphasize, with this example, the importance of bi-dimensional simulation of semiconductor devices , in the investigation of dimensional effects of sub-microns devices, which cannot be expected by the classical Shockley theory[13].

## 8. CONCLUSIONS

This paper details the bi-dimensional simulation of MOSFET devices in thermal equilibrium condition. A classical bi-dimensional doping profile is presented, and the discretization and numerical techniques for the determination of the potential distribution are extensively explored. The importance of the Poisson equation in the understanding of MOSFET dimensional effects is underlined, with a classical example of threshold voltage variation in a short-channel device.

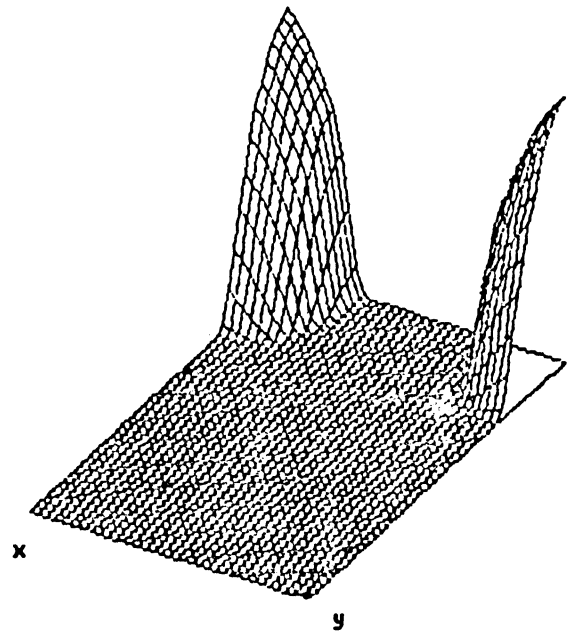


Figure 5: Doping concentration of $1.0\mu m$ device ($cm^{-3}$)

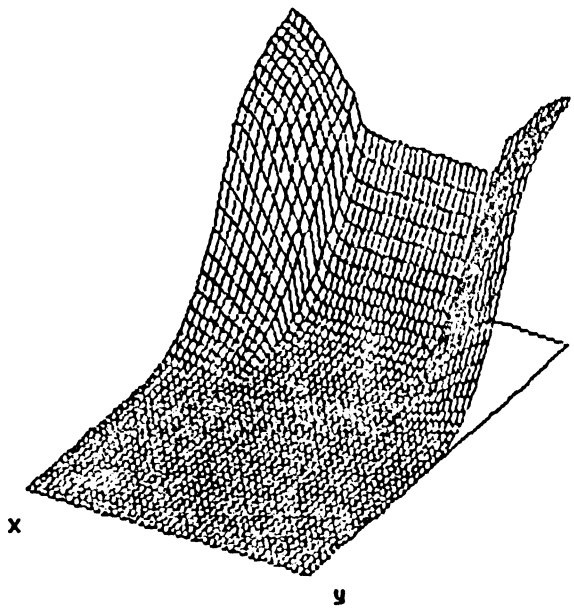


Figure 6: Electrical potential of $5.0\mu m$ device (V)

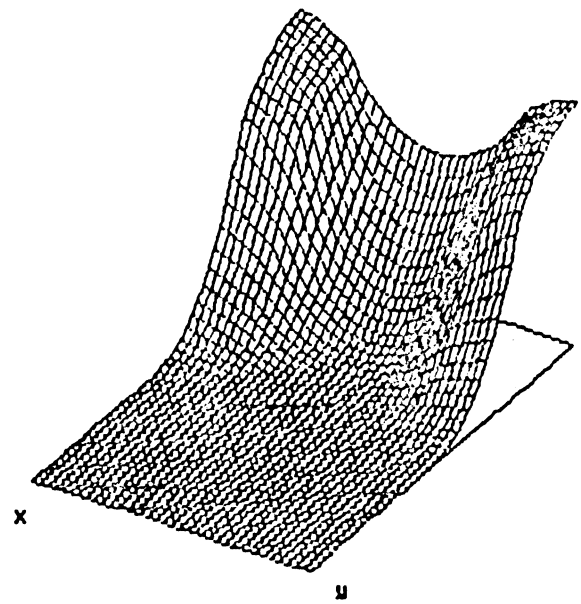


Figure 7: Electrical potential of $1.0\mu m$ device (V)

## 9. ACKNOWLEDGMENTS

This work was supported in part by a grant of Conselho Nacional de Desenvolvimento Científico e Tecnológico (CNPq), Process number: 131.894/87-0. The authors are grateful to A. G. Figueiredo Filho for the suggestions done during the computation of figures.

## 7. REFERENCES

1. Siegfried Selberherr, *Analysis and Simulation of Semiconductor Devices*, Springer-Verlag, April 1984,

2. D. Antoniadis, S. Hansen, R. Dutton, *SUPREM II - A Program for IC Process Modeling and Simulation*, Stanford Electron. Lab., CA, Tech. Rep. 5019-2, 1978

3. S. Selberherr, A, S. Schutz, H. W. Potzl, *MINIMOS - A Two-Dimensional MOS Transistor Analyzer*, IEEE J. Solid-State Circuits, vol. SC-15, pp. 605–614, 1973.

4. E. M. Buturla, P. E. Cottrell, B. M. Grossman, K. A. Salsburg, *Finite-element Analysis of Semiconductor Devices: The Fielday Program*, IBM T. Res. Dev., vol. 25, pp. 218–231, 1981.

5. H. K. Gummel, *A Self-Consistent Interative Scheme for One-Dimensinal Steady State Transistor Calculations*, pp. 455–465, October 1964,

6. A. De Mari, *An Accurate Numerical Steady-State One Dimensional Solution of The p-n Junction*, Solid-State Electron., vol. 11 pp. 33–58, 1967.

7. D. L. Sharfetter, H. K. Gummel, *Large-Signal Analysis of a Silicon Read Oscillator*, IEEE Trans. Electron Devices, vol. ED-, pp. 64–77, January 1969,

8. M. S. Mock, *A Two-Dimensional Mathematical Model of Insulated-Gate Field-Effect Transistor*, Solid-State Electron., vol. 16 pp. 601-609–,. 1972

9. H. Craslaw, J. Jaeger, *Conduction of Heat in Solids*, 1959.

10. Hee-Gook Lee, J. D. Sansbury, R. W. Dutton, J. L. Moll, *Modeling and Measurement of Surface Impurity Profiles of Laterally Diffused Regions*, IEEE J. Solid-State Circuits, vol. SC-13, pp. 455–461, 1976.

11. Hee-Gook Lee, R. W. Dutton, *Modeling and Measurement of Surface Impurity Profiles of Laterally Diffused Regions*, IEEE Trans. Electron Devices, vol. ED-28, pp. 1136–1147, 1981.

12. J. F. Gibbons, W. S. Mylroie, S. W. Mylroie, *Projected Range Statistics*, Strandsberg: Halstead Press, 1975

13. W. Shockley, *A Unipolar Field-effect Transistor*, Proc. IRE,pp. 1365–1377, November 1952,